

Supporting Information for:

The Rhodamine–Perylene Compact Electron
Donor–Acceptor Dyad: Spin–Orbit Charge–Transfer
Intersystem Crossing and the Energy Balance of
the Triplet Excited States

Muhammad Imran,[†] Dongyi Liu, [†] Kaiyue Ye, Xue Zhang and Jianzhang Zhao^{*}

State Key Laboratory of Fine Chemicals, Frontiers Science Center for Smart Materials
Oriented Chemical Engineering, School of Chemical Engineering, Dalian University of
Technology, E-208 West Campus, 2 Ling Gong Rd., Dalian 116024, P. R. China.

E-mail: zhaojzh@dlut.edu.cn

[†] These authors contributed equally to this work.

Contents

| | |
|---|-----|
| 1. General Information..... | S3 |
| 2. Molecular Structure Characterization Data..... | S3 |
| 3. UV–Vis Absorption Spectra and Fluorescence Spectra..... | S6 |
| 4. Singlet Oxygen Quantum Yields..... | S8 |
| 5. Electrochemical Study..... | S9 |
| 6. Nanosecond Time-resolved Transient Absorption Spectra..... | S10 |

1. General Information

All the chemicals used in synthesis are analytically pure and were used as received. Solvents in reactions were dried and distilled prior to use. ^1H and ^{13}C NMR spectra were recorded on the Bruker Avance spectrometers (400 MHz). ^1H and ^{13}C NMR chemical shifts are reported in parts per million (ppm) relative to TMS, with the residual solvent peak used as an internal reference. The mass spectra were measured by HRMS (ESI).

2. Molecular Structure Characterization Data

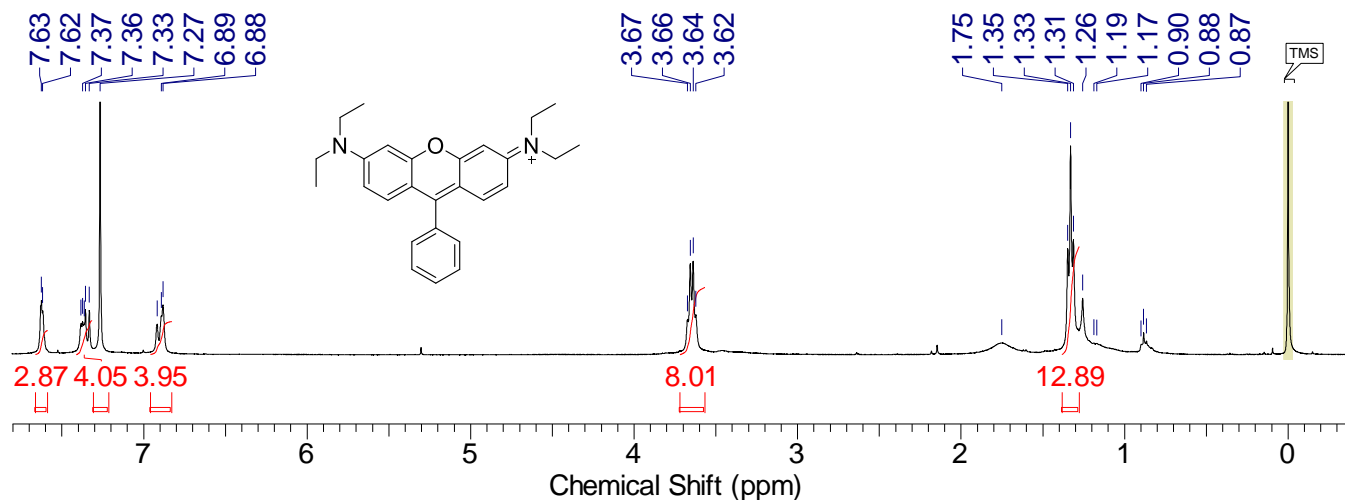


Figure S1. ^1H NMR spectrum of RB-Ph (CDCl_3 , 400 MHz).

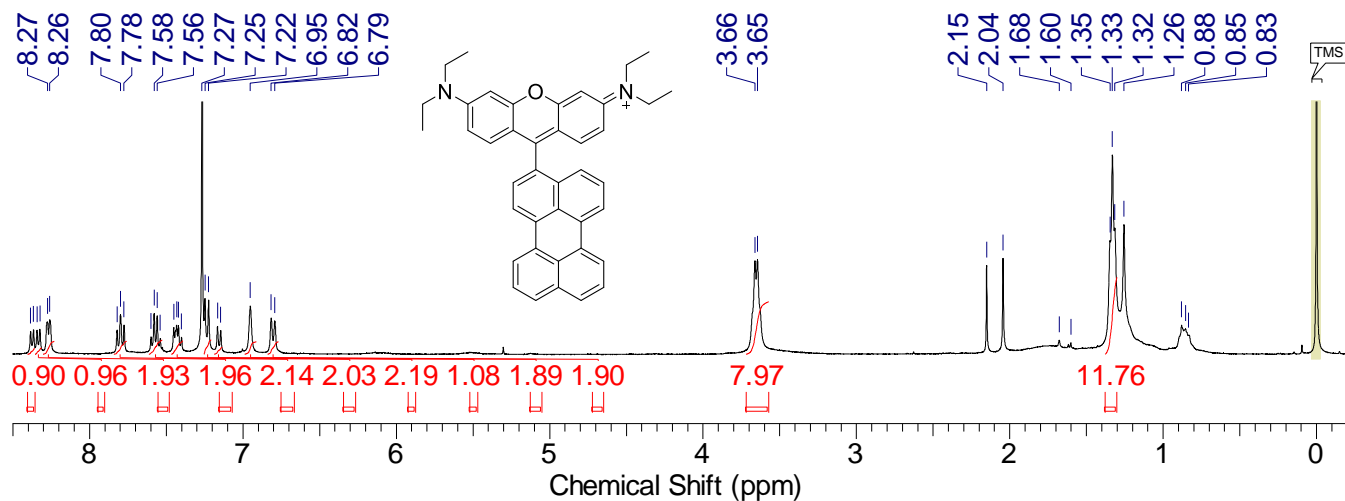


Figure S2. ^1H NMR spectrum of RB-Pery (CDCl_3 , 400 MHz).

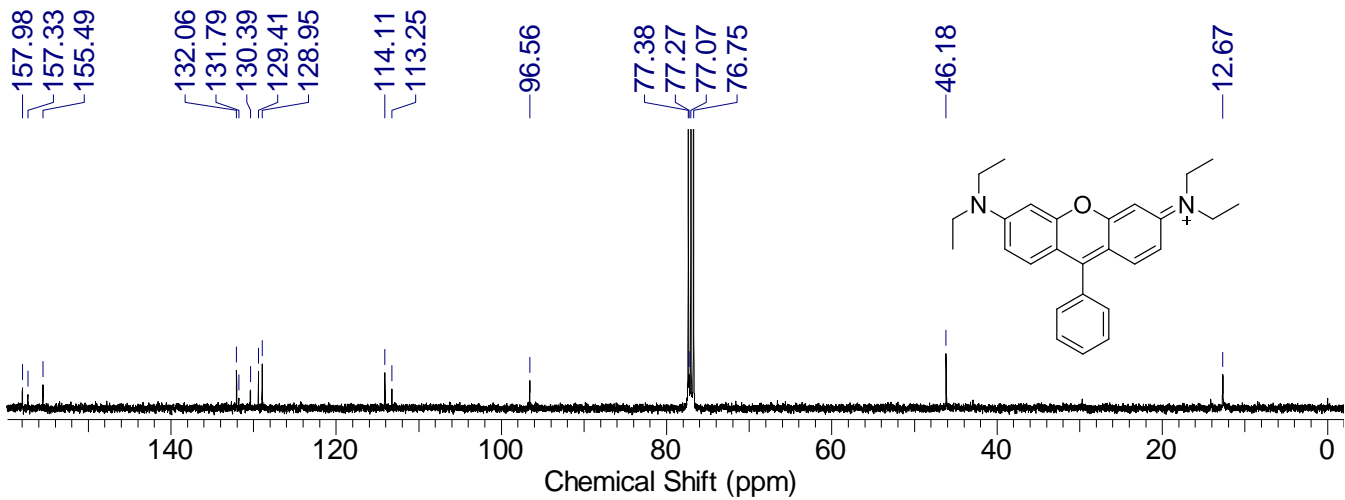


Figure S3. ¹³C NMR spectrum of RB-Ph (CDCl_3 , 126 MHz).

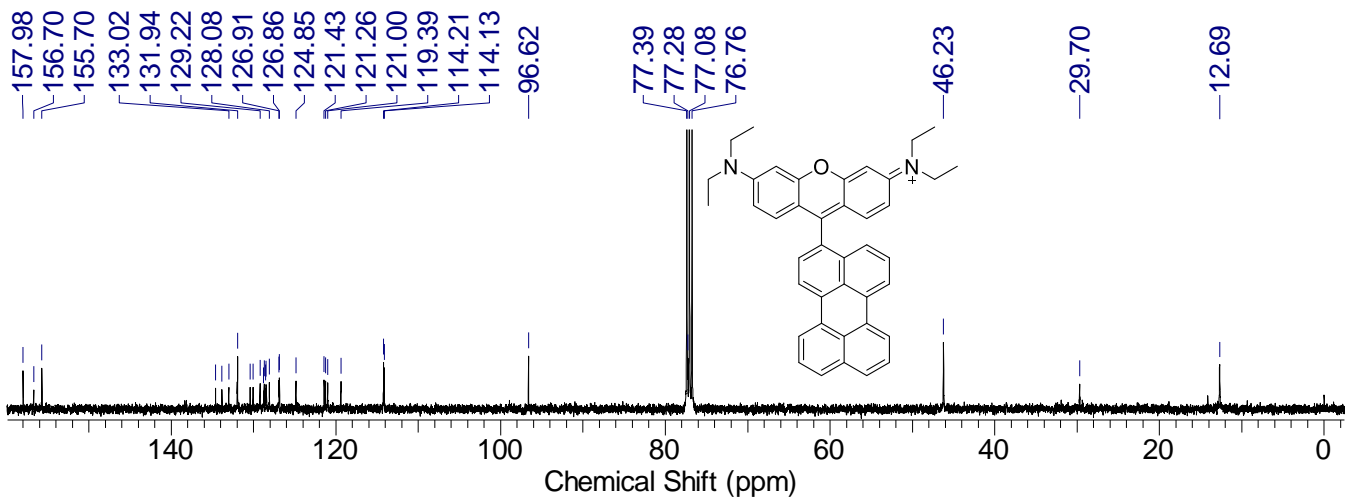


Figure S4. ¹³C NMR spectrum of RB-Pery (CDCl_3 , 126 MHz).

20191029-LDY-M573- #4-5 RT: 0.03-0.05 AV: 2 SB: 2 0.02-0.03 NL: 4.88E6
T: FTMS + p ESI Full ms [120.00-1000.00]

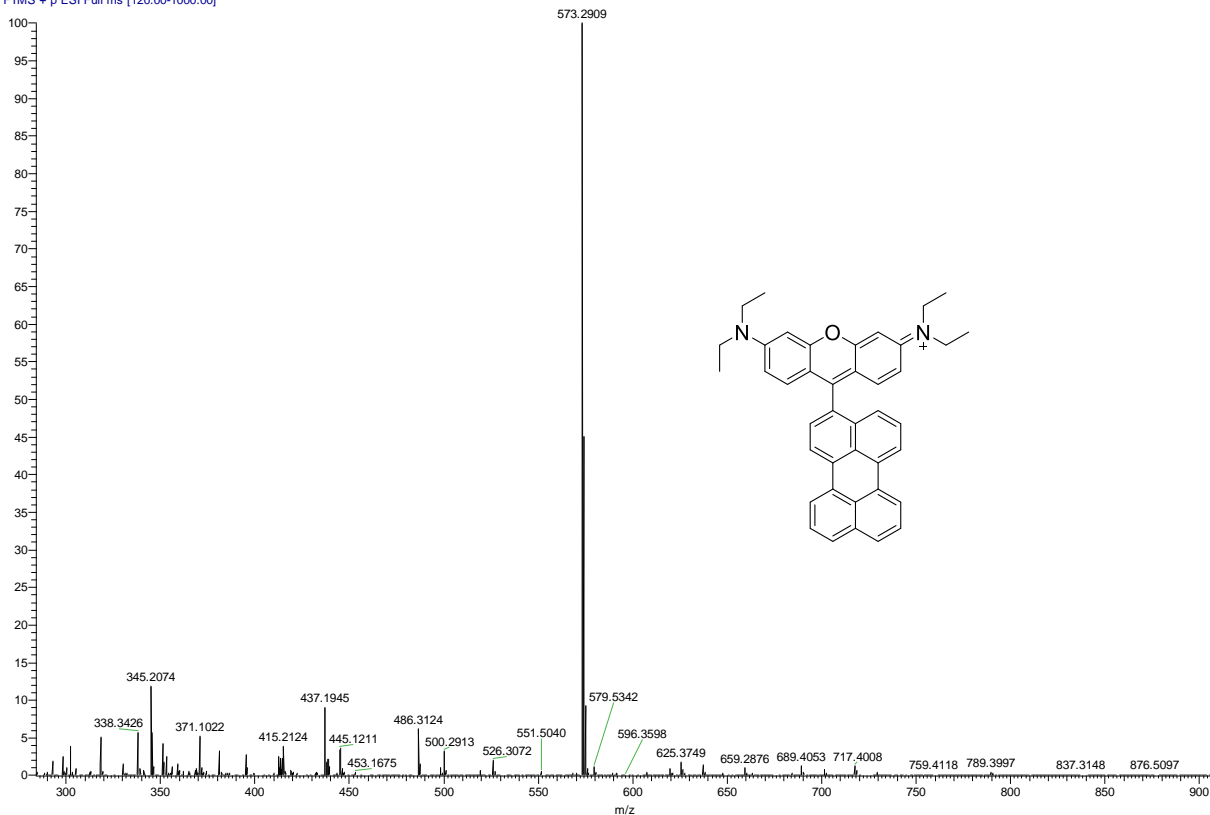


Figure S5. ESI-HRMS of RB-Pery.

3. UV-vis Absorption and Fluorescence Emission Spectra

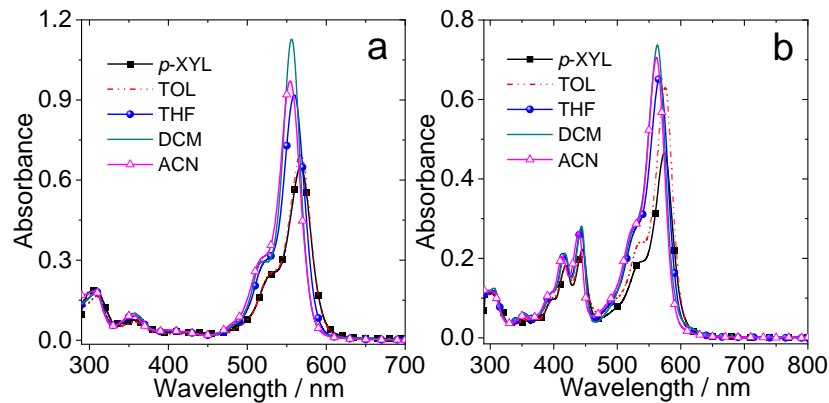


Figure S6. UV-vis absorption spectra of compound (a) RB-Ph and (b) RB-Pery in different solvents. $c = 1.0 \times 10^{-5}$ M.

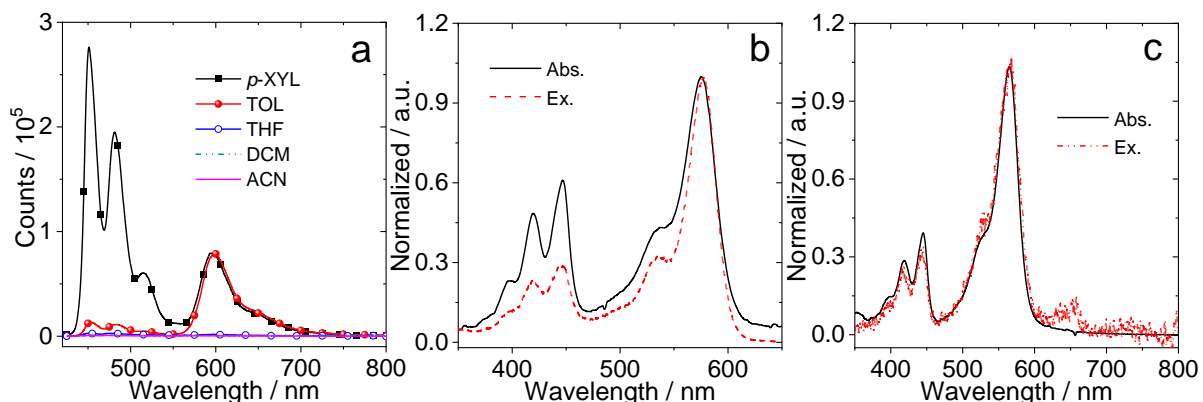


Figure S7. (a) Fluorescence emission spectra (optically-matched solutions were used, $A = 0.10$) of RB-Pery in different polarity solvents, $\lambda_{\text{ex}} = 415$ nm. Normalized UV-vis absorption and fluorescence excitation spectra of RB-Pery (b) in *p*-XYL monitored at 650nm and (c) in DCM monitored at 800 nm. $c \approx 1.0 \times 10^{-5}$ M. 25 °C.

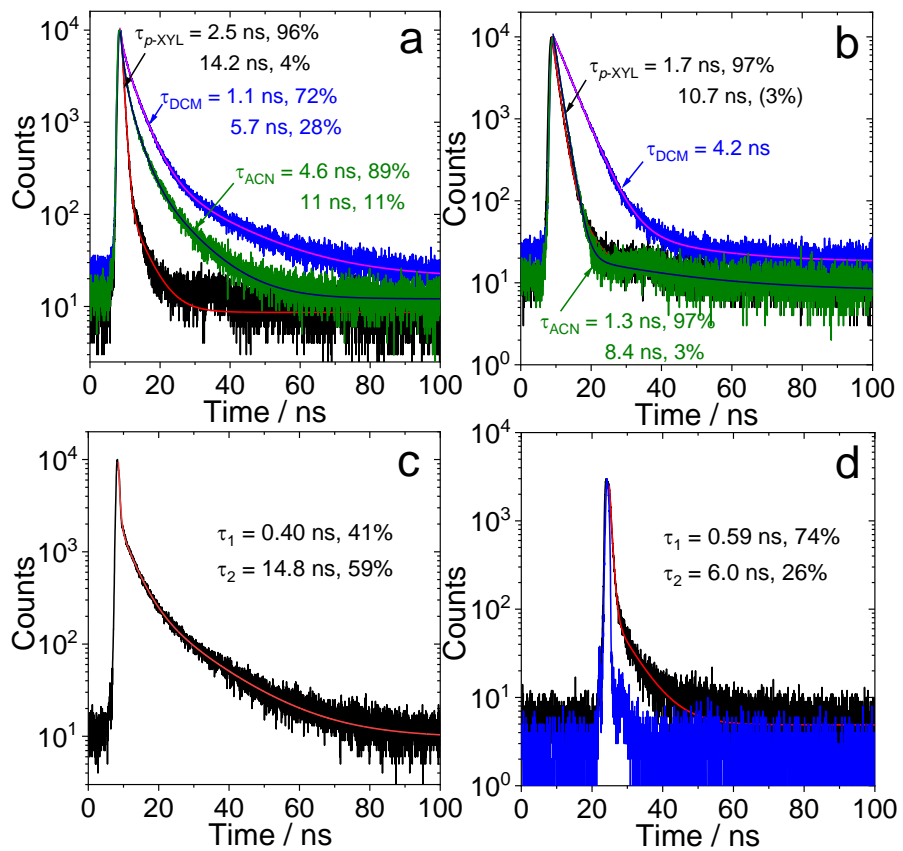


Figure S8. Fluorescence decay traces of the compounds in different solvents (a) RB-Pery monitored at 585 nm and (b) RB-Ph monitored at 585 nm. Fluorescence decay trace of the RB-Pery in DCM (c) monitored at 630 nm and (d) monitored at 690 nm. Excited with a 405 nm picosecond pulsed laser. $c \approx 1.0 \times 10^{-5}$ M. 25 °C.

Table S1. Absolute Photo-luminescence Quantum Yield of the Compounds in different solvents^a

| Compounds | <i>p</i> -XYL | TOL | THF | DCM | ACN |
|-----------|-------------------|-------------------|----------------|----------------|----------------|
| Pery | 75.5% | 77.7% | 75.0% | 82.2% | 77.0% |
| RB-Ph | 12.9% | 14.2% | 28.8% | 71.9% | 21.0% |
| RB-Pery | 7.0% ^b | 2.4% ^b | — ^d | — ^d | — ^d |
| | 6.1% ^c | 6.0% ^c | | | |

^a Error bar: ± 0.1 , Pery and RB-Ph ($\lambda_{\text{ex}} = 415$ nm), RB-Pery ($\lambda_{\text{ex}} = 506$ nm), $A = 0.10$, 25 °C. ^b Excitation at perylene moiety. ^c Excitation at rhodamine moiety. ^d Not observed.

Table S2. Luminescence Lifetime of the Compounds in different solvents ^a

| Compounds | <i>p</i> -XYL (ns) | TOL (ns) | THF (ns) | DCM (ns) | ACN(ns) |
|-----------|--------------------|----------------|-----------------|----------------|-----------------|
| Pery | 4.0 ± 0.3 | 3.9 ± 0.3 | 4.2 ± 0.3 | 4.5 ± 0.3 | 4.3 ± 0.4 |
| RB-Ph | 1.7 (97%) | 1.3 (97%) | 2.6 ± 0.3 | 4.2 ± 0.3 | 1.6 ± 0.3 |
| | 10.7 (3%) ± 0.2 | 8.5 (3%) ± 0.2 | | | |
| RB-Pery | 2.5 (96%) | 3.3 (96%) | 3.8 (37%) | 1.1 (72%) | 4.6 (89%) |
| | 14.2 (4%)± 0.2 | 16.7 (4%)± 0.2 | 10.4 (63%)± 0.3 | 5.7 (28%)± 0.2 | 11.0 (11%)± 0.2 |

^a $C = 1.0 \times 10^{-5}$ M, $\lambda_{ex} = 405$ nm, 25 °C. The values in the table are in %.

4. Singlet Oxygen Quantum Yields

Table S3. Singlet Oxygen Quantum Yields of Compounds in Different Solvents ^a

| Compounds | <i>p</i> -XYL (33.5) | TOL (33.9) | THF (37.4) | DCM (41.1) | ACN (46.0) |
|-----------|----------------------|----------------|----------------|----------------|----------------|
| Pery | 4.8 ± 0.5 | 3.0 ± 0.5 | 8.2 ± 1 | 4.0 ± 0.5 | 16.2 ± 1 |
| RB-Ph | — ^b | — ^b | — ^b | — ^b | — ^b |
| RB-Pery | 8.0 ± 1 | 2.7 ± 0.5 | — ^b | — ^b | — ^b |

^a Rose Bengal was used as standard ($\Phi_\Delta = 76\%$ in MeOH) for RB-Ph and RB-Pery, Ru(bpy)₃(PF₆)₂ was used as standard ($\Phi_\Delta = 57\%$ in DCM) for Pery, the values are in %. The values in parenthesis are the E_T (30) values of the solvents, in kcal mol⁻¹. ^b Not observed.

5. Electrochemical Study

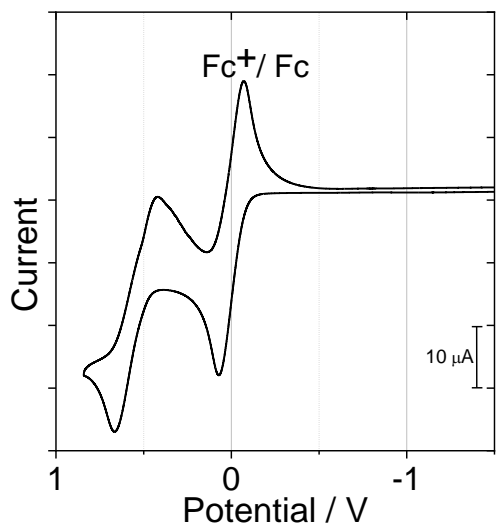


Figure S9. Cyclic voltammogram of perylene. Conditions: in deaerated DCM containing 0.10 M Bu_4NPF_6 as supporting electrode, Ag/AgNO_3 as reference electrode, redox potentials are *versus* Fc/Fc^+ . Scan rates: 50 mV/s. $c = 1.0 \times 10^{-3}$ M. 25 °C.

6. Nanosecond Transient Absorption Spectroscopy

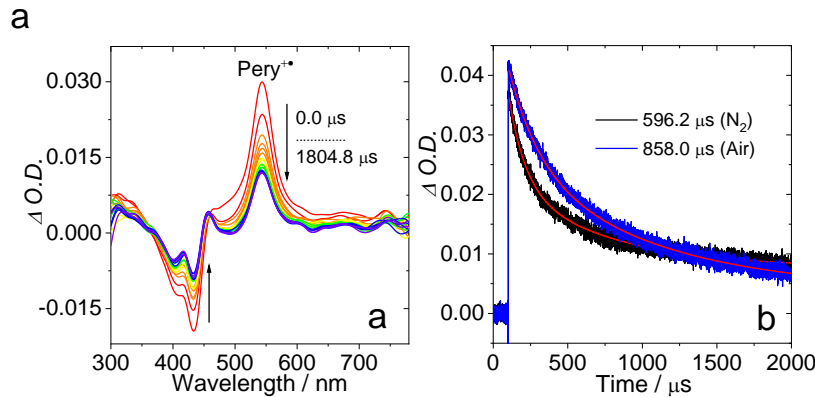


Figure S10. (a) Transient absorption spectra of Pery in deaerated DCM and (b) decay traces at 540 nm in DCM, $c = 2.0 \times 10^{-5}$ M, $\lambda_{\text{ex}} = 432$ nm. 25 °C.

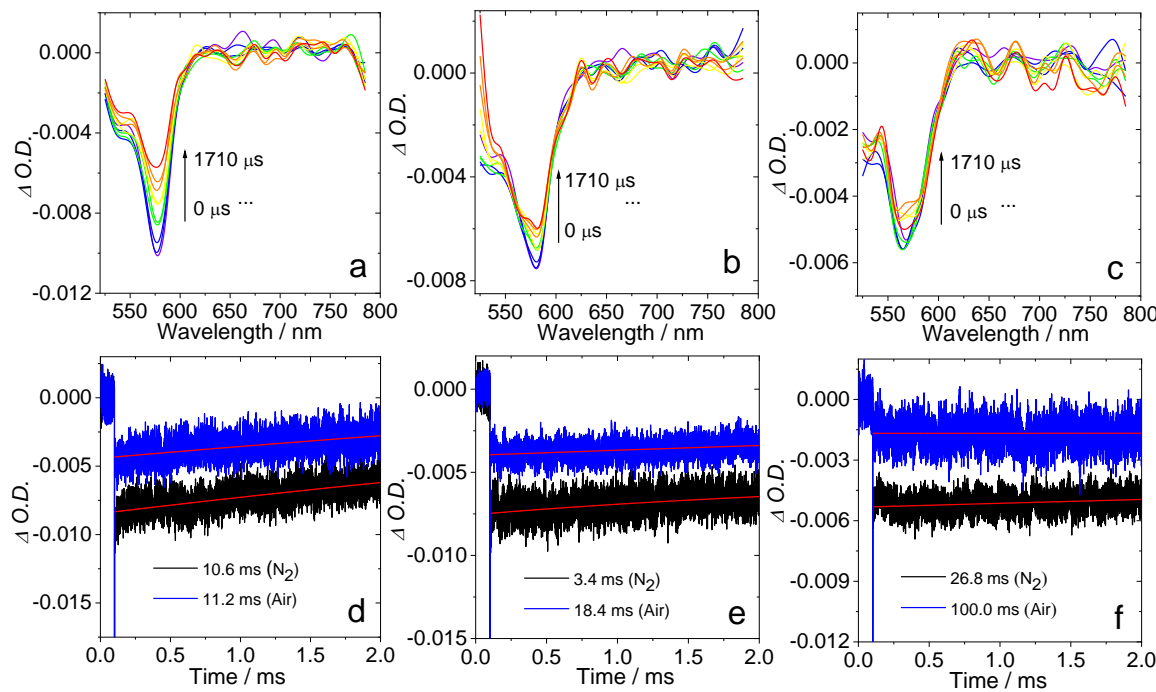


Figure S11. Transient absorption spectra of RB-Pery, (a) in deaerated *p*-XYL, $c = 1.0 \times 10^{-5}$ M; (b) in deaerated TOL, $c = 1.0 \times 10^{-5}$ M; (c) in deaerated THF, $c = 2.0 \times 10^{-5}$ M; (d-f) respective decay traces at 575 nm under aerated and deaerated conditions. $\lambda_{\text{ex}} = 570$ nm. 25 °C.

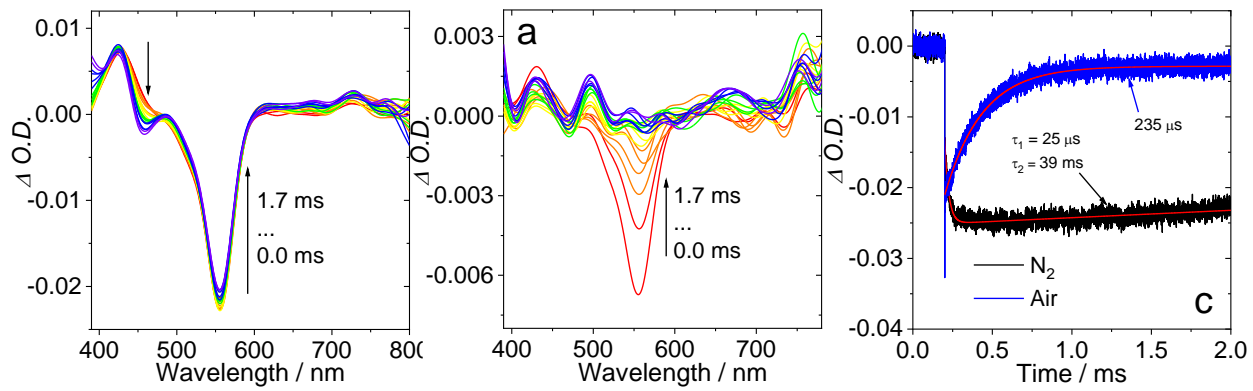


Figure S12. Transient absorption spectra of RB-Ph ($c = 1.0 \times 10^{-4}$ M) upon adding TEA ($c = 4.0 \times 10^{-3}$ M) (a) in deaerated DCM, (b) in aerated DCM and (c) decay traces at 560 nm in both cases. $\lambda_{ex} = 550$ nm. 25 °C.

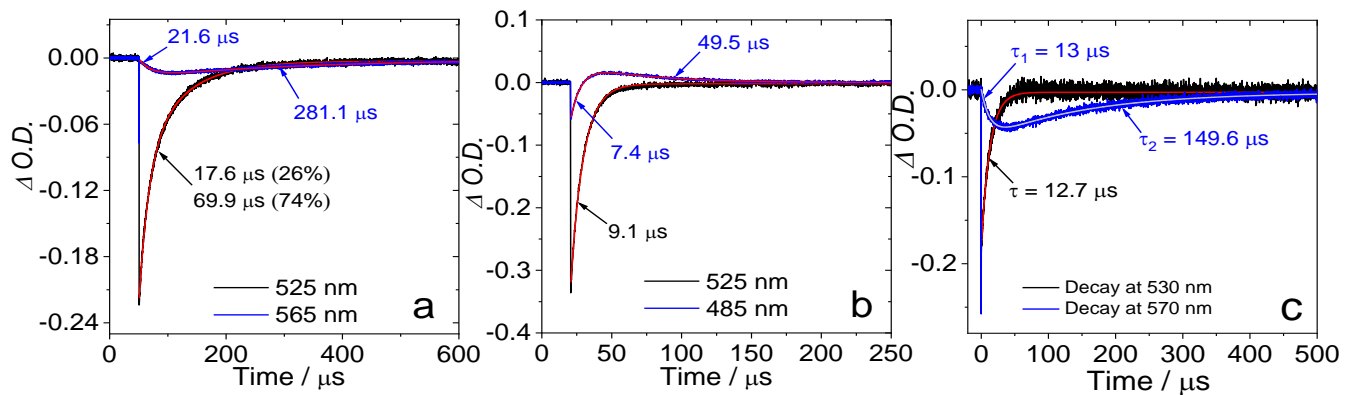


Figure S13. Intermolecular triplet-triplet energy transfer (TTET): from diiodo-BDP to RB-Ph, Pery and RB-Pery measured by ns-TA spectroscopy; (a) selected kinetic traces of the mixture of the ns-TA spectra of diiodo-BDP and RB-Ph. (b) selected kinetic traces of the mixture of the ns-TA spectra of diiodo-BDP and Pery. (c) selected kinetic traces of the mixture of the ns-TA spectra of diiodo-BDP and RB-Pery. The concentration of diiodo-BDP was fixed $c[\text{diiodo-BDP}] = 5.0 \times 10^{-6}$ M and 1:1 molar ratios were used in every case. The ns-TA spectra are given in the main text. In deaerated ACN, $\lambda_{ex} = 520$ nm. 25 °C.

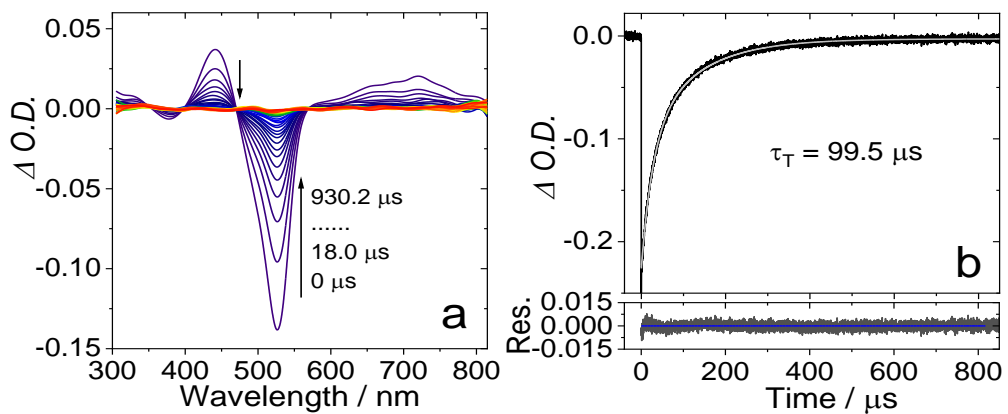


Figure S14. (a) Nanosecond transient absorption spectra of diiodo-BDP and (b) decay trace at 530 nm; $c = 5.0 \times 10^{-6}$ M in deaerated ACN. $\lambda_{\text{ex}} = 520$ nm. 25 °C.

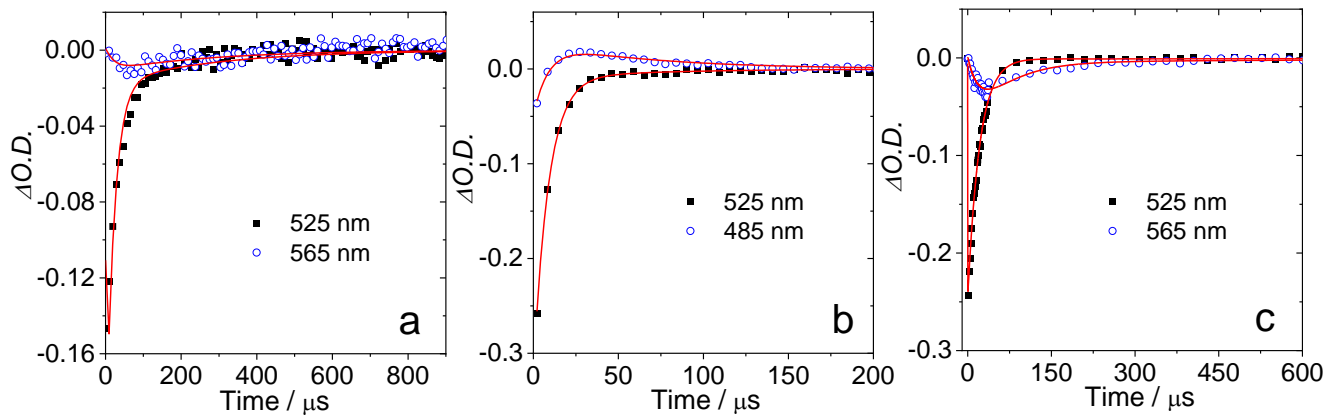


Figure S15. Selected kinetic decay traces obtained after global fitting analysis (a) from ns-TA data of diiodo-BDP/RB-Ph mixture (b) from ns-TA data of diiodo-BDP/Pery mixture and (c) from ns-TA data of diiodo-BDP/RB-Pery. The respective raw data and SADS spectra are given in the main text Figure 6 and 7.